Наносистеми, наноматеріали, нанотехнології
Nanosistemi, Nanomateriali, Nanotehnologii
2022, т. 20, № 1, сс. 15–23

PACS numbers: 73.21.Fg, 73.40.Lq, 73.63.Hs, 81.07.St, 85.35.Be

Theoretical Study of the Conduction Band and Energy Gap of GaInNAs/InP Quantum Well Structure

Hassan T. B. ALHammade

College of Science,
Al Muthanna University,
66001 Al Samawa City, Iraq

Changes of temperature and composition play a major role in enhancement of the electronic properties of low-dimensional semiconductor devices. Therefore, the interest of researchers in this field is increased. In this article, we study the effect of both the temperature and the nitrogen ratio on the electronic structure of $Ga_xIn_{1-x}N_yAs_{1-y}/InP$ quantum well. The band anticrossing model, Varshni model, and Bose–Einstein model are adopted to determine the nitrogen effect on conduction band (E_- and E_+). The band gap of $Ga_xIn_{1-x}As$ as ternary alloy, and band offsets (ΔE_c, ΔE_v) for the $Ga_xIn_{1-x}N_yAs_{1-y}/InP$ quantum wells are estimated as functions of nitrogen content and temperature. The splitting of conduction band into two non-parabolic subbands due to adding the nitrogen to GaInAs alloy contributes into increase of the band offset of $Ga_xIn_{1-x}N_yAs_{1-y}/InP$ quantum well, and thus, into increase of the number of energy states inside the quantum well. The results may be useful for applications in electronic and optical devices.

Зміни температури та складу відіграють важливу роль у поліпшенні електронних властивостей низьковимірних напівпровідникових пристроїв. Тому інтерес дослідників до цієї сфери підвищується. У цій статті ми вивчаємо вплив як температури, так і Нітроґенового співвідношення на електронну структуру квантової ями $Ga_xIn_{1-x}N_yAs_{1-y}/InP$. Модель антиперетинання зон, модель Варшні та модель Бозе–Айнштайна прийнято для визначення ефекту Нітроґену на зону провідности (E_- і E_+). Ширина забороненої (енергетичної) зони для $Ga_xIn_{1-x}As$ як тернарного стопу та зонні зміщення (ΔE_c, ΔE_v) для квантових ям $Ga_xIn_{1-x}N_yAs_{1-y}/InP$ оцінюються як функції вмісту Нітроґену та температури. Розщеплення зони провідности на дві непараболічні підзони за рахунок додавання Нітроґену до стопу GaInAs сприяє збільшенню зміщенню зони квантової ями $Ga_xIn_{1-x}N_yAs_{1-y}/InP$, і, таким чином, збільшенню кількости енергетичних станів всередині квантової ями. Результати можуть бути корисні для застосувань в електронних і оптич-

них пристроях.

Key words: $Ga_xIn_{1-x}N_yAs_{1-y}$/InP quantum well, conduction band, band anticrossing, band offset.

Ключові слова: квантова яма $Ga_xIn_{1-x}N_yAs_{1-y}$/InP, зона провідности, антиперетинання зон, зміщення зони.

(Received 25 March, 2021)

1. INTRODUCTION

GaInAs/InP is a semiconductor material formed of elements that fall into Group III and V of the periodic table [1]. Indium phosphide (InP) is a binary compound with a zinc blende (ZB) structure, has direct band gap energy about 1.35 eV and 1.425 eV at 300 K and 0 K, respectively. It is an important semiconductor material and is used as a base for high speed electrical and optoelectronic devices [2–5]. Dilute group arsenide–nitride compound semiconductors, such as GaAsN and GaInAsN, attracted the interest of many researchers [6]. The band gap energy *versus* lattice parameter relation for GaInAsN, GaInAs, InP, and GaAs is shown in Fig. 1 [7]. The InGaAsN/InP QW have been applied as waveguide diode lasers, and diode lasers emitting [6].

In this study, we start by examining the conduction band and electron effective mass effect with the presence of nitrogen content of GaInNAs alloy by the BAC model. Next, it is explained the band gap of GaInAs and GaInNAs alloys as function of temperature and

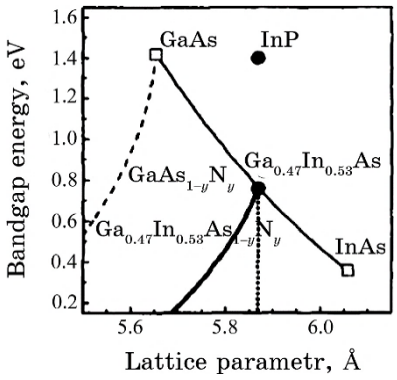

Fig. 1. Band gap energy *versus* lattice parameter of GaAsN, GaInAs and GaInAsN calculated within the framework of the BAC model for an interaction parameter C_{NM} derived in this work. The dotted line indicates the band gap of GaInAsN lattice matched to InP.

nitrogen content by means of the use of Varshni and Bose–Einstein models. Then, we calculate the band offsets and energy states for the GaInNAs/InP and GaInAs/InP quantum well (QW) structures. Finally, there are discussed the advantages of temperature and nitrogen content effects on the electronic properties of GaInNAs/InP and GaInAs/InP quantum well structures.

2. THEORETICAL PART

An anticrossing interaction between the narrow band of localized nitrogen states and the extended conduction-band states of semiconductor alloys can be treated using perturbation theory, leading to the following eigenvalue equation [8, 9]:

$$\begin{vmatrix} E_N - E_M & V_{MN} \\ V_{MN} & E_M - E_N \end{vmatrix} = 0 . \tag{1}$$

The solution to this eigenvalue problem gives us the dispersion relation for the dilute nitride:

$$E_{\pm}(\mathbf{k}) = \frac{1}{2}\left\{ E_N + E_M(\mathbf{k}) \pm \left[\left(E_N - E_M(\mathbf{k}) \right)^2 + 4V_{MN}^2 \right]^{\frac{1}{2}} \right\}, \tag{2}$$

where

$$E_M(\mathbf{k}) = E_g^{(\mathrm{GaInAs})} + \frac{\hbar^2 k^2}{2m^*} . \tag{3}$$

For $\mathbf{k} = \mathbf{0}$,

$$E_M(T) = E_g^{(\mathrm{GaInAs})} = E_g(0) - \frac{\alpha T^2}{T + \beta}, \tag{4}$$

and

$$E_M(T) = E_g^{(\mathrm{GaInAs})} = E_g(0) - \frac{2a_B}{e^{\frac{\theta_B}{T}} - 1}, \tag{5}$$

where E_M and E_N are the energies of the unperturbed conduction band edge and of the N level relative to the top of the valence band, respectively, and V_{MN} is the matrix element of the term describing the interaction and hybridization between localized N states and the extended states.

We have gathered all the parameters necessary for band anticrossing (BAC) modelling in Table 1.

TABLE 1. Parameters used for calculations within the framework of the BAC model.

Parameters	Value	Refs.
E_N	1.64	[9]
V_{NM}	$C_{NM}\sqrt{y}$	[9]
C_{NM}	2.7	[10, 12]

TABLE 2. The values of the important parameters, which are within the Varshni and Bose–Einstein expressions.

	$E(0)$, eV	α, eV/(K·10^{-4})	β, K	$E(0)$, eV	a_B, eV	θ_B, K	Refs.
GaInNAs	1.067 (0.961)	6	500	1.063 (0.957)	0.137	360	[9]
GaInAs	1.347 (1.221)	6	300	1.346 (1.22)	0.07	180	[9]
InP	1.425 (1.35)	—	—	—	—	—	[3]

$$E_{\pm}(\mathbf{k}) = \frac{1}{2}\left\{\left(E_N + E_g^{(\mathrm{GaInAs})} + \frac{\hbar^2 k^2}{2m^*}\right) \pm \left[\left(E_N - E_g^{(\mathrm{GaInAs})} + \frac{\hbar^2 k^2}{2m^*}\right)^2 + 4V_{MN}^2\right]^{\frac{1}{2}}\right\}. \quad (6)$$

Within the Varshni model [11, 15],

$$E_g(T) = E_g(0) - \frac{\alpha T^2}{T+\beta}, \quad (7)$$

where $E_g(0)$ is the energy gap at absolute zero, T is an absolute temperature, and

$$E_{\pm}(T) = \frac{1}{2}\left\{\left(E_N + E_g(0) - \frac{\alpha T^2}{T+\beta}\right) \pm \left[\left(E_N - \left(E_g(0) - \frac{\alpha T^2}{T+\beta}\right)\right)^2 + 4V_{MN}^2\right]^{\frac{1}{2}}\right\}. \quad (8)$$

Constants β and α have the values listed in Table 2.

Within the Bose–Einstein model [13, 14],

$$E_g(T) = E_g(0) - \frac{2a_B}{e^{\frac{\theta_B}{T}} - 1}, \quad (9)$$

where $\theta_B = E/k_B$ is the temperature of the phonon oscillator.

$$E_{\pm}(T) =$$

$$= \frac{1}{2}\left\{\left(E_N + E_g(0) - \frac{2a_B}{e^{\frac{\theta_B}{T}} - 1}\right) \pm \left[\left(E_N - \left(E_g(0) - \frac{2a_B}{e^{\frac{\theta_B}{T}} - 1}\right)\right)^2 + 4V_{MN}^2\right]^{\frac{1}{2}}\right\}. \quad (10)$$

The electron effective mass m_e^* for the GaInNAs is much greater than that for the GaInAs with the same In concentration, and increases as the N concentration increasing up to 1% [17]. It can be evaluated as in Ref. [19] from the dispersion relations displayed in Eq. (2),

$$m_e^* = 2m_e^{*(\mathrm{GaInAs})}\left[1 + \frac{\left|E_N - E_g\right|}{\left(E_N - E_g\right)^2 + 4V_{MN}^2}\right]. \quad (11)$$

3. RESULTS AND DISCUSSION

According to the BAC model, the interaction between the highly localized nitrogen states (E_N) and the extended conduction band states for the host GaInAs semiconductor matrix leads to a splitting of the conduction band into energy states (E_- and E_+) as illustrated in Fig. 2. Figure 2 shows a distinct flattening of the conduction band E_- for energies approaching the E_N (for $k \approx 0.15\pi/a$). For comparison, the unperturbed GaInAs conduction band and the position of the nitrogen level are shown.

Figure 3 shows dispersion relations for the conduction E_+ and E_-

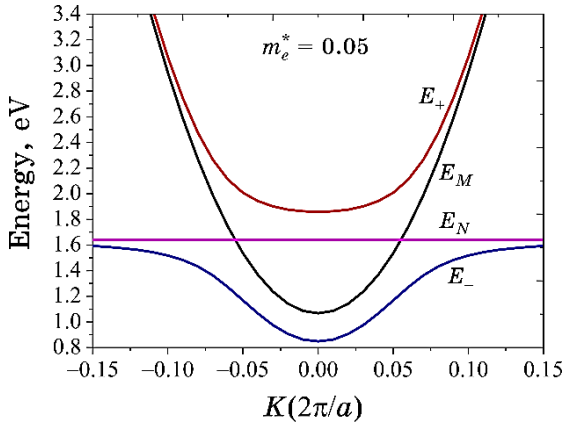

Fig. 2. BAC-model $E(\mathbf{k})$-band plots at 300 K.

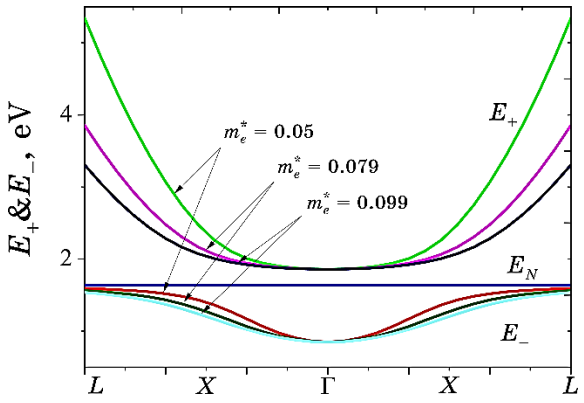

Fig. 3. Calculated dispersion relations E **(k)** and E_+**(k)** for $Ga_xIn_{1-x}N_yAs_{1-y}$ for three different electron effective masses.

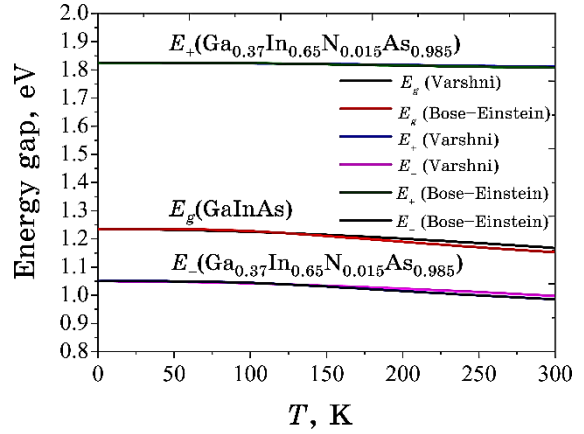

Fig. 4. The theoretical temperature dependence of the band-gap energy E_g, E_+, and E_- for $Ga_xIn_{1-x}N_yAs_{1-y}$/InP QW at different nitrogen ratios ($y = 0$, 0.015) by the Varshni and B–E formulas in the range 0–300 K. The upper and under curves are calculated with Eqs. (7) and (10), whereas the middle curves are calculated by Eqs. (7) and (9).

subbands for $Ga_xIn_{1-x}N_yAs_{1-y}$ at different electron effective masses. The strength of anticrossing interaction between the localized and delocalized states varies across the different conduction-band minima (points X, L, Γ), changing the fundamental nature of the gap. As noted from Figure 3, the conduction E_+ and E_- subbands at the Γ-point **(k = 0)** is not changed with increasing electron effective mass, and on the contrary, at X and L points.

The theoretical temperature dependence of the E_+ and E_- energies for $GaxIn_{1-x}N_yAs_{1-y}$ alloy at different nitrogen ratios in the range

0–300 K is shown in Fig. 4.

The energy gap of semiconductors tends to reduce as the temperature is increased. This behaviour can be better understood, if we consider that the interatomic spacing is expanded due to the amplitude of the atomic vibrations increased because of the increasing of thermal energy. This effect is specified by the linear expansion coefficient of the material; however, the increase of interatomic spacing will reduce the potential between the electrons in the material that, in turn, reduces the value of the energy gap. Temperature dependence of energy gap, E_g, in $Ga_xIn_{1-x}As$ alloy (middle curves) was calculated by means of the Varshni and B–E formulas.

Nitrogen-content dependence of E_- and E_+ transitions is shown in Fig. 5. The results in Fig. 5 show a dramatic difference in the N-composition dependence of the low-energy E_- and E_+ transitions at the Γ point. The E_- and E_+ transitions show a very strong, nonlinear dependence on the N content. The lines show the calculated dependences for E_- and E_+ using the BAC model.

The calculated band offsets (ΔE_c, ΔE_v) for N-containing system

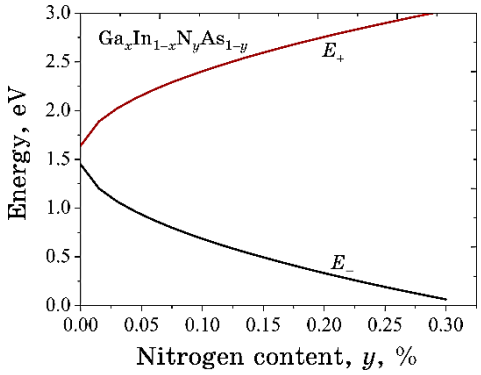

Fig. 5. Nitrogen-composition dependence of E_- and E_+ energies. The curves represent the BAC-model predictions for $Ga_xIn_{1-x}N_yAs_{1-y}$/InP QW.

TABLE 3. Calculated band offsets (ΔE_c, ΔE_v) for $Ga_xIn_{1-x}N_yAs_{1-y}$/InP QW at different temperatures ($T = 0$ K, 300 K) and the nitrogen content ($y = 0$, 0.015%).

y, %	T, K	ΔE_c, meV	ΔE_v, meV
0	0	25	53
	300	41	88
0.015	0	115	244
	300	124	256

TABLE 4. Bound state energies of the 10 nm thickness $Ga_xIn_{1-x}N_yAs_{1-y}$/InP QW at 300 K calculated using the finite well model.

Quantum number, n	Electron energy e_n, meV	Heavy hole hh_n, meV	Light hole hl_n, meV
1	23	13	48
2	92	52	192
3	—	117	—
4	—	208	—

TABLE 5. Bound state energies of the 10 nm thickness $Ga_xIn_{1-x}As$/InP QW at 300 K calculated using the finite well model.

Quantum number, n	Electron energy e_n, meV	Heavy hole hh_n, meV	Light hole hl_n, meV
1	17.6	6	31
2	—	25	—
3	—	56	—

QW and another N-free QW are shown in Table 3. The effect of both temperature and nitrogen on the band offset is strongly observed. As seen from Table 3, the band offsets are increased with an increase in both temperature and nitrogen content in $Ga_{0.37}In_{0.63}N_{0.015}As_{0.985}$ and $Ga_{0.37}In_{0.63}As$ alloys. This leads to an increase in the energy states inside the quantum well that, in turn, leads to an improvement in the electronic and optical applications of the devices. This result is agreed with [18].

For comparison between N-containing system QW and another N-free QW, the bound state energies [in meV units] for both systems at room temperature are shown in Tables 4 and 5, respectively.

4. CONCLUSION

This study has shown that nitrogen has a large effect on the conduction band structure. The results show that the addition of a few percent of N into GaInAs to form GaInNAs alloys leads to reducing the energy gap close to the Γ point. In addition, the dispersion relations show effective mass independent on electrons especially at the points Γ and L. In contrast, there are shown its temperature dependence. The band offsets also are affected by an increase of nitrogen content. This one leads to an increase of the bound states inside the $Ga_xIn_{1-x}N_yAs_{1-y}$/InP quantum well. Consequently, the transported charge carriers in the well are increased, and this one leads to improving the performance of the devices.

REFERENCES

1. E. Herbert Li, *IEEE Journal of Quantum Electronics*, **34**, No. 6: 982 (1998); doi:10.1109/3.678594
2. H. Burkhard, H. W. Dinges, and E. Kuphal, *Journal of Applied Physics*, **53**, No. 1: 655 (1982); https://doi.org/10.1063/1.329973
3. R. Ahuja et al., *Solid State Communications*, **104**, No. 5: 249 (1997); https://doi.org/10.1016/S0038-1098(97)00287-1
4. J. Mudron et al., *ASDAM'98. Conference Proceedings. Second International Conference on Advanced Semiconductor Devices and Microsystems (Cat. No. 98EX172)* (IEEE: 1998); doi:10.1109/ASDAM.1998.730207
5. N. P. Siwak, X. Z. Fan, and R. Ghodssi, *Journal of Micromechanics and Microengineering*, **25**, No. 4: 043001 (2015); https://doi.org/10.1088/0960-1317/25/4/043001
6 J. Wagner et al., *16th IPRM. 2004 International Conference on Indium Phosphide and Related Materials* (IEEE: 2004); doi:10.1109/ICIPRM.2004.1442604
7. D. Serries et al., *Conference Proceedings. 14th Indium Phosphide and Related Materials Conference (Cat. No. 02CH37307)* (IEEE: 2002); doi:10.1109/ICIPRM.2002.1014449
8. W. Shan et al., *Journal of Applied Physics*, **86**, No. 4: 2349 (1999); https://doi.org/10.1063/1.371148
9. R. J. Potter et al., *physica status solidi (a)*, **187**, No. 2: 623 (2001); https://doi.org/10.1002/1521-396X(200110)187:2<623::AID-PSSA623>3.0.CO;2-Q
10. S. Procz et al., *Journal of Applied Physics*, **103**, No. 7: 073103 (2008); https://doi.org/10.1063/1.2895002
11. Sajal Paul, J. B. Roy, and P. K. Basu, *Journal of Applied Physics*, **69**, No. 2: 827 (1991); https://doi.org/10.1063/1.348919
12. Czeslaw Skierbiszewski, *Semiconductor Science and Technology*, **17**, No. 8: 803 (2002); https://doi.org/10.1088/0268-1242/17/8/309
13. S. A. Lourenço et al., *Journal of Applied Physics*, **89**, No. 11: 6159 (2001); https://doi.org/10.1063/1.1367875
14. R. Kudrawiec et al., *Acta Physica Polonica. Series A: General Physics*, **106**, No. 2: 249 (2004).
15. T. H. Chen, Y. S. Huang, D. Y. Lin, and K. K. Tiong, *Journal of Applied Physics*, **96**, No. 11: 6298 (2004); https://doi.org/10.1063/1.1805724
16. Katsuhiro Uesugi, Ikuo Suemune, Tatsuo Hasegawa, Tomoyuki Akutagawa, and Takayoshi Nakamura, *Applied Physics Letters*, **76**, No. 10: 1285 (2000); https://doi.org/10.1063/1.126010
17. Z. Pan, L. H. Li, Y. W. Lin, B. Q. Sun, D. S. Jiang, and W. K. Ge, *Applied Physics Letters*, **78**, No. 15: 2217 (2001); https://doi.org/10.1063/1.1362335
18. Beşire Gönül, Koray Köksal, and Ebru Bakír, *Physica E: Low-Dimensional Systems and Nanostructures*, **31**, No. 2: 148 (2006); https://doi.org/10.1016/j.physe.2005.11.007
19. Marta Gladysiewicz, Robert Kudrawiec, and Marek S. Wartak, *IEEE Journal of Quantum Electronics*, **51**, No. 5: 1 (2015); doi:10.1109/JQE.2015.2410340